Shell-type micromechanical oscillator

Maxim Zalalutdinov*[a], Keith Aubin[b], Christopher Michael[d], Rob Reichenbach[b],
Tuncay Alan[c], Alan Zehnder[c], Brian Houston[e], Jeevak Parpia[a], Harold Craighead[b]

[a]Physics, [b]Applied and Engineering Physics, [c]Theoretical & Applied Mechanics Departments;
Cornell University, Ithaca, NY, USA
[d]Physics Department, University of Illinois at Urbana-Champaign, IL, USA
[e]Naval Research Laboratory, Washington DC, USA

ABSTRACT

Shell-type micromechanical resonators operating in the radio frequency range were fabricated utilizing mechanical stress that is built into polysilicon thin films. A significant increase of the resonant frequency (compared to flat, plate-type resonators of the same size) and the rich variety of vibrating modes demonstrate great potential for "2.5-Dimensional" MEMS structures. A finite curvature of the shell also provides a novel mechanism for driving resonators by coupling in plane stress with out of plane deflection. By modulating the intensity of a low power laser beam (P~10μW) focused on the resonator we introduced a time-varying, in-plane, thermomechanical stress. This stress modulation resulted in experimentally observed, large amplitude, out-of-plane, vibrations for a dome-type resonator.
A double laser beam experimental setup was constructed where mechanical motion of a shell-type resonator was actuated by a sharply focused, modulated Ar^{+} ion (blue) laser beam and detected by a red HeNe laser using an interferometric setup. A positive feedback loop was implemented by amplifying the red laser signal (related to the oscillator deflection) and using it to modulate the blue (driving) laser beam. Stable self-sustained vibrations were observed providing that the feedback gain was high enough. Employing a frequency selective amplifier in the feedback loop allowed excitation of different modes of vibrations. Fine frequency tuning was realized by adjusting the CW component of either lasers' intensity or a phase shift in the feedback loop. Frequency stability better than 1 ppm (10^{-6}) at 9 MHz was demonstrated for self-sustained vibrations for certain modes of the dome-shaped oscillators.

Keywords: Shell, resonator, thermal drive, positive feedback, self-sustained oscillations, frequency stability

1. INTRODUCTION

The development of radio frequency microelectromechanical systems (RF MEMS) is largely motivated by possible applications in wireless communication devices[1]. High quality, miniature and CMOS-technology compatible MEMS resonators are seen as an attractive alternative to existing RF passive components. In contemporary RF devices frequency-determining elements are implemented in two major ways. The first requires microfabrication of capacitors and inductors on-chip. Even though they consume the major part of the IC "real estate" and exhibit a low quality factor[2] Q~50, on-chip LC circuits are widely used for GHz-range devices. On the other hand, quartz crystals, surface acoustic wave (SAW) filters, ceramic filters and high-Q LC go the other way – they are implemented as stand-alone elements and create a bottleneck for future miniaturization of RF devices. Their high quality factor (Q~10^6 for quartz resonators and Q~10^5 for ceramic SAW filters) plus high temperature stability, both indispensable features for wireless devices, force RF designers accept these off-chip components. This approach conflicts with modern trends in wireless systems, especially with smart dust[3]-type projects, which require a radio-on-chip to be implemented with the smallest size and for the lowest price.

Micromechanical resonators as frequency-determining elements are expected to be the key for the radio-on-chip project. Modern surface micromachining tools[4] allow fabrication of suspended silicon structures with a fundamental frequency of mechanical vibrations, f_0, in the RF range[5,6]. The MEMS resonator quality factor Q~10^4 is few order of

---

magnitude superior compared to LC circuits. Detailed study of the physical mechanism of the energy dissipation[7,8,9] in MEMS resonators results in a further improved quality factor[10,11], steadily approaching that of a single-crystal quartz resonator. This progress should enable the incorporation of MEMS based signal generators and frequency standards into nearly any RF device.

The natural approach for building such a generator is to implement the MEMS resonator as a frequency determining element in the feedback loop of an amplifier and to provide conditions for self-sustained oscillations. The strain energy $kx^2/2$, stored in a MEMS resonator can be comparable to electric energy $LI^2/2$ in a conventional inductor. However, methods to convert the electrical signal into mechanical motion of the resonator (drive) and back (detection) represent the major challenge in RF MEMS design. Piezoelectric transduction requires piezoelectric materials incompatible with CMOS technology. Magnetomotive methods for driving and detection used to demonstrate the highest resonant frequency in MEMS[6] rely on high magnetic field and low temperatures.

It has been demonstrated that micromechanical reference oscillators can be operated using electrostatic drive and detection[12,13,14]. However, capacitive methods are difficult to implement: relatively high voltage is required and narrow gap capacitors for both drive and detection impose significant restrictions on the design. Both oscillators[12,13] employ beam-like geometry resulting in relatively low quality factor $Q \sim 10^3$. Problems related to cross-talk between drive and detection can be severe. The phase noise for either of these devices is significantly higher than one would expect from similar quartz-based oscillators and both groups attribute this extra phase noise to capacitive transduction problems. This motivates ongoing search for new design of micrmechanical resonators and novel drive-detection methods .

In this paper we describe a MEMS oscillator based on the shell-type resonator and employing a thermomechanical drive concept. Our dome-type resonators, which can be regarded as a spherical shell clamped on the outside were fabricated from polysilicon film and demonstrate a quality factor of $Q \sim 9,000$ at the resonant frequency $f_0 \sim 9MHz$. Using a focused Ar^+ blue laser beam we demonstrate that in-plane thermomechanical stress due to local heating can result in significant out-of-plane motion of the shell and provides an effective driving mechanism. Employing the second laser beam (red HeNe) as an interferometry-based detection tool we demonstrate all-optical operation of the shell resonator.

A frequency generator was built by closing a positive feedback loop: the amplified signal acquired by the red (read-out) laser was amplified, phase shifted and applied as a modulation on the blue (driving) laser beam intensity. Self-sustained oscillations were demonstrated with the frequency up to 9MHz, based on different modes of the shell vibrations.
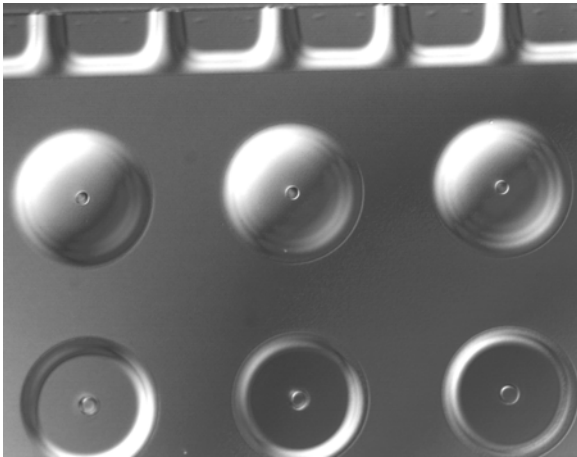

Fig.1 DIC micrograph of the dome-shape resonators

2. FABRICATION

As a first step of fabrication, 1 μm of thermal oxide was grown on a surface of [100] silicon wafers. This oxide was used later as a sacrificial layer. Polycrystalline silicon film was deposited on the surface of the oxide by low pressure chemical vapor deposition (LPCVD) method at 590°C. After the deposition the wafer was annealed for 15 min. at 1050°C. E-beam lithography with following dry etch were then used to create 8μm-diameter holes through the top

polysilicon layer. After stripping off the resist the structure was dipped into concentrated hydrofluoric acid (HF 49%). Dissolving the sacrificial silicon dioxide (etch rate ~1μm/min) results in a suspended membrane-like structure with a hole at the center. The etching time determines the outer diameter of the cavity underneath the polysilicon film. If the polysilicon were stress-free, the released membrane would be flat. However, significant compressive stress incorporated in polysilicon film as a result of deposition and annealing parameters makes the planar configuration unstable and leads to a buckled membrane. The resulting structure has a dome shape with a hole at the top. Fig. 1 shows optical micrograph obtained by DIC (Differential Interference Contrast, known also as Nomarsky contrast). An array of three domes, with outer diameter 60μm is shown in the central part of the picture. Three other membranes on the bottom line buckled down and are stuck to the substrate. Presence of high compressive stress in polysilicon film is clearly demonstrated by ripples on the ledge (top part of the picture). Considering the early stage of the undercut process it is easy to see that buckle-up configuration is favorable. In fact, using critical point dry (CPD) process to avoid surface tension we could reach 100% yield for dome-type resonators.

3. EXPERIMENTAL SETUP

The interferometric technique[15] is a natural choice for the detection of the motion of the dome resonator because the thin polysilicon shell and wafer create a Fabry-Perot interferometer. Fig.2 shows reflection coefficient R for 630nm light wavelength as a function of the gap h between the released membrane and the substrate. The strong periodic dependence $R(h)$ allows us to detect oscillatory motion of the resonator by measuring the AC component of the reflected light intensity. A HeNe laser beam was focused by an objective lens onto a 2μm spot size on the dome's surface. The same lens was used to collect the reflected light. A Nonpolarizing beam splitter (1) was used to direct the reflected laser beam to a wideband photodetector. Another beam splitter (2) and white light source provided an optical image of the structure. One can position the laser beam on any spot of interest by monitoring this image on the microscope screen.
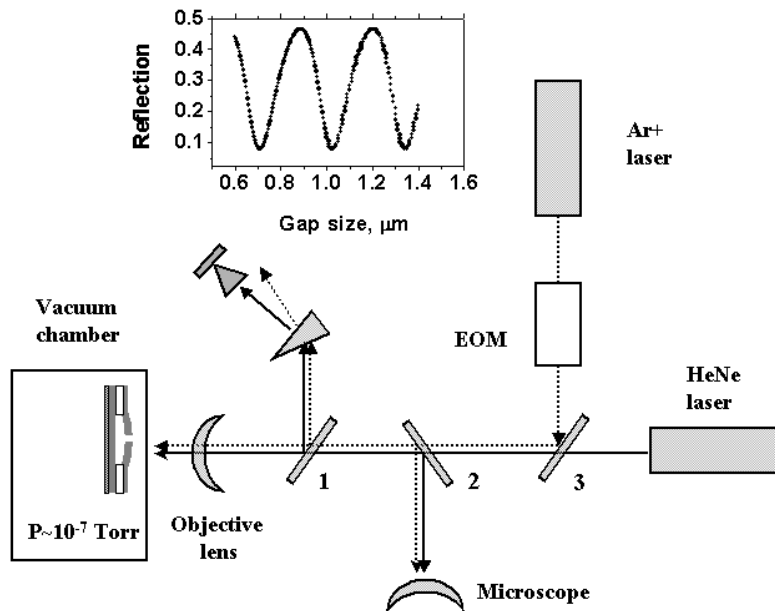

Fig.2 Experimental setup

The second laser (Ar+) was included in the experimental setup for experiments with light-driven MEMS resonators. By employing a system of mirrors and a beamsplitter (3), the blue laser beam is directed through the same objective lens, focused into a 2μm spot and can be positioned independently of the red (HeNe) laser beam. The intensity of the Ar^+ laser can be controlled by Electro Optical Modulator (OEM) with an 80MHz bandwidth. An additional dispersing prism was mounted in front of the photodetector to avoid saturation by the blue laser.

The sample was mounted inside an ion pump-based vacuum system (P<10^{-7} Torr) with a fused silica window for optical access.

4. THERMOMECHANICAL DRIVE

The double beam configuration of the experimental setup allows an all-optical operation of the shell-type resonator. The dome exhibits a large amplitude out-of-plane vibration (detected using the red laser) when heated by the blue laser, modulated at the resonant frequency. The physical mechanism for the laser drive is related to the thermomechanical stress created by the focused laser beam within the shell. Figure 3 illustrates the result of finite element analysis (FEA) for the temperature distribution within the shell (a) and the shell deformation (b) caused by the local thermal expansion. The absorption of 50μW laser power induces a 0.85K temeperature increase at the beam spot. For the flat membrane case such a local overheating would build up an in-plane stress but would be too small to create an out-of-plane buckling. In contrast here, due to the 3-Dimensional nature of the dome oscillator the thermal stress is free to be released by the out-of-plane deformation. Static deflection caused by a 50μW laser beam is estimated to be 0.3nm (fig.3b). The corresponding amplitude of the in-resonance vibrations would be enhanced up to 3μm by the quality factor of the resonator Q~10^4 if it were not limited by non-linear effects.

It should be emphasized that according to our calculations the light pressure effect on the dome shape is negligible (five orders of magnitude weaker than the thermal stress drive).
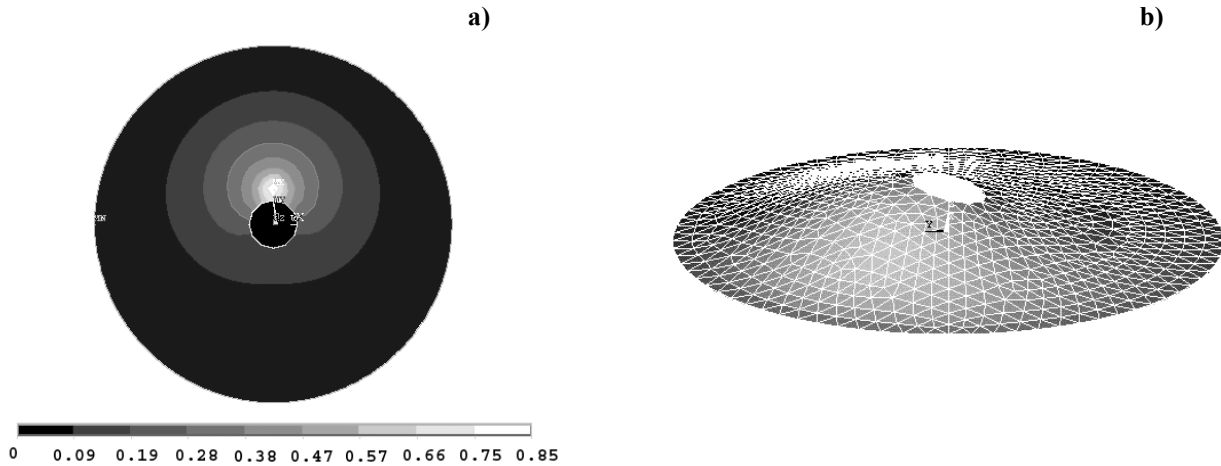
a)   b)


```
0    0.09  0.19  0.28  0.38  0.47  0.57  0.66  0.75  0.85
```

Fig. 3 Thermal distribution (a) and deformed shape (b) for the shell heated by a 50μW laser beam

The all-optical operation of the micromechanical resonators greatly simplifies design of the device, eliminating the need for metallization, capacitive pick-up electrodes, piezoelements etc The bare silicon resonator can be exposed to a wide range of temperatures or corrosive atmospheres while preserving full functionality.

4. VIBRATING MODES

The driving-detection technique that is implemented by two independently positioned laser beams provides a tool to enable the identification of the resonator's modes. Since the excitation by the driving beam is provided locally, in a point-like manner, one can raster the spot of the detecting (red) laser across the structure and build a map of the phase shift between the driving signal and detected motion for every particular location. For a circular symmetrical structure like the dome or a disc resonator it is natural to assume that the excited mode will have a maximum at the driving laser beam location. Superimposing the detecting laser over the driving beam should produce an in-phase signal. As the red laser's spot is displaced from the position of the blue laser spot, it may traverse a nodal diameter or a circular node (depending on the particular excited mode). At that point the phase shift between the driving signal and the detected motion will change by 180°, which can be readily detected by a network analyzer. In a real experiment it is more convenient to move the drive laser beam and preserve the alignment of the detecting beam with the photodetector. Fig. 4

shows the phase plots acquired for the different laser beams locations over the disc oscillator illustrating 180º phase shift.
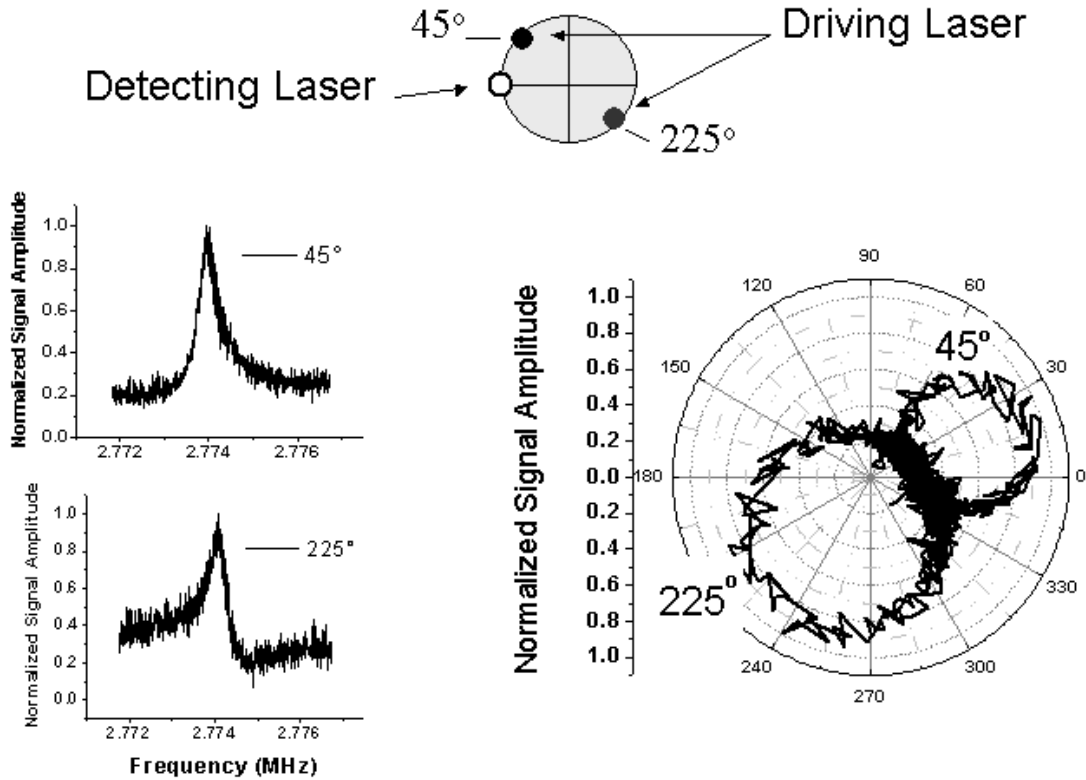

Fig. 4 Resonance peaks in rectangular and polar coordinates illustrating 180º phase shift for diametrically-opposite locations of the driving beam.

This mode recognition technique, applied to the dome-type resonators allowed us to identify four low frequency modes γ_{11}, γ_{01}, γ_{21} and γ_{02}. Experimental values for the resonant frequencies and quality factors for these and higher modes are collected in Table 1. The shape of the modes for the dome resonator, obtained by FEA, are shown by Fig. 5. The resonator was modeled as a spherical shell with outer diameter 60 um, 8μm inner hole diameter, 0.25 μm polysilicon film thickness, 1.3 mm dome height. Shell elements were used for modal analysis. The remaining stress was neglected.

Mode	f, MHz	Q
γ_{11}	3.66	8240
γ_{01}	4.08	4350
γ_{21}	5.48	8365
γ_{02}	6.98	9720
	9.78	9000

By taking into account the center of mass motion for the different modes of the dome's vibration we attribute the observed difference in a quality factors to the clamping losses.

γ_{11} $\qquad$ γ_{01}

γ_{21} $\qquad$ γ_{02}
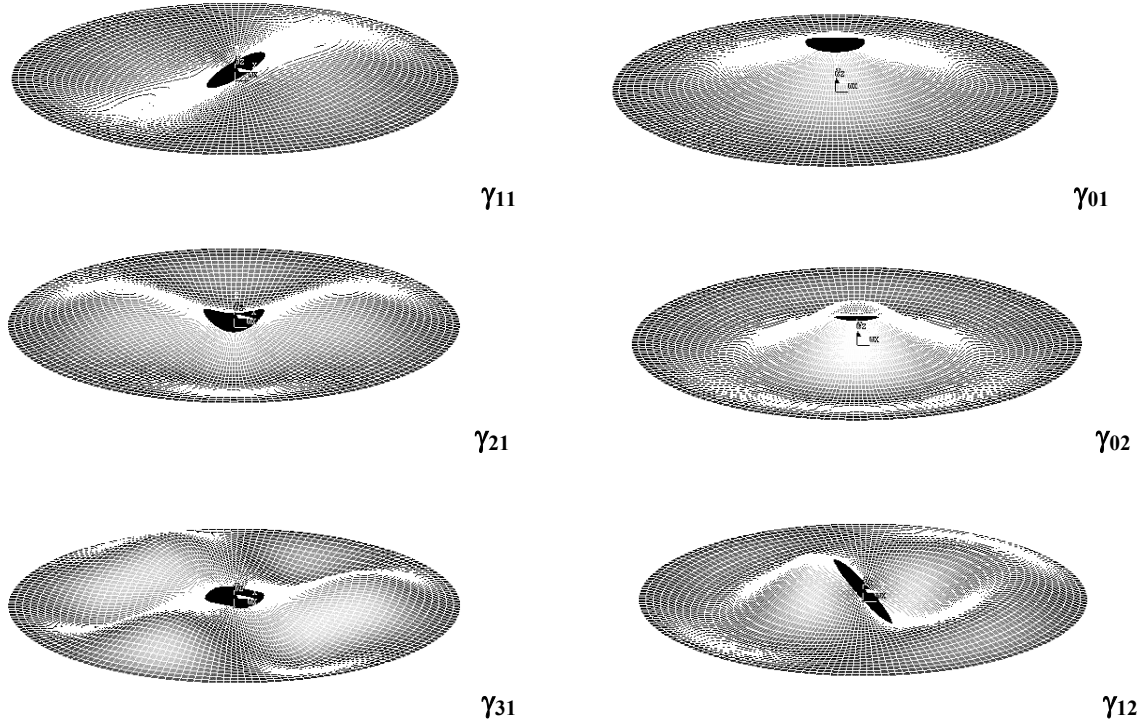
γ_{31} $\qquad$ γ_{12}

Fig. 5 Modes of vibrations (arranged by the increase of the resonant frequency) for the dome resonator.

5. FREQUENCY GENERATOR

Positive feedback was closed by amplifying the AC voltage from the photodetector and applying the resulting signal as a modulation of the driving beam intensity. The block diagram of the resulting generator is shown in Fig.7. The tunable amplifier MATEC615 (Gain 120dB, Q=20) and high voltage amplifier (ENI, broadband gain 150dB) in series provide sufficient gain to ensure access to the self-oscillatory regime. The tunability of the MATEC615 amplifier allows the excitation of selected modes from the spectrum of the dome oscillator in the frequency region up to 27MHz. It should be emphasized that since $Q_{amplifier} << Q_{resonator}$, the operation of the generator is determined solely by the MEMS component.

For the 60μm outer diameter dome we could attain the self-oscillatory regime for any of the 5 modes listed in table 1. The best performance in terms of frequency stability was achieved employing the highest, 9.3MHz mode. Due to the nonlinearity of the interferometric detection technique, higher harmonics are always present in the spectrum of the signal acquired from the photodetector.

A 12 digit frequency counter (measuring time 100ms) was used to monitor the frequency stability of the generator output. Time record of the counter read-out, shown in Fig.6, demonstrates <0.8ppm standard deviation for the frequency values measured over a 3 minute interval. The long-time drift (line fit in Fig.6) is attributed to the mechanical drift of the laser spot over the dome.

The high stability of the optically operated MEMS generator can be readily utilized in a setup that employs a MEMS resonator as a sensor. Easily converted to a digital form, the frequency output carries information on added mass[16], periodic force[17] or force gradient[18] affecting the resonator.

Applications the shell-type MEMS resonators in RF wireless devices stimulate ongoing research that will enable the integration of a dome oscillator into CMOS environment. The project includes an implementation of the described thermomechanical actuation with the laser beam replaced by a microWatt power, microfabricated local Joule heater. Full CMOS-integrated version of the MEMS frequency generator with capacitive pick-up ant thermal drive is expected as a result of the project.
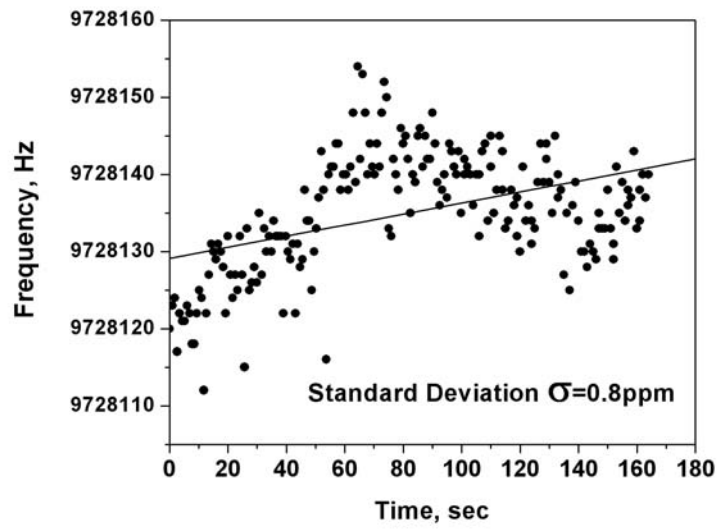
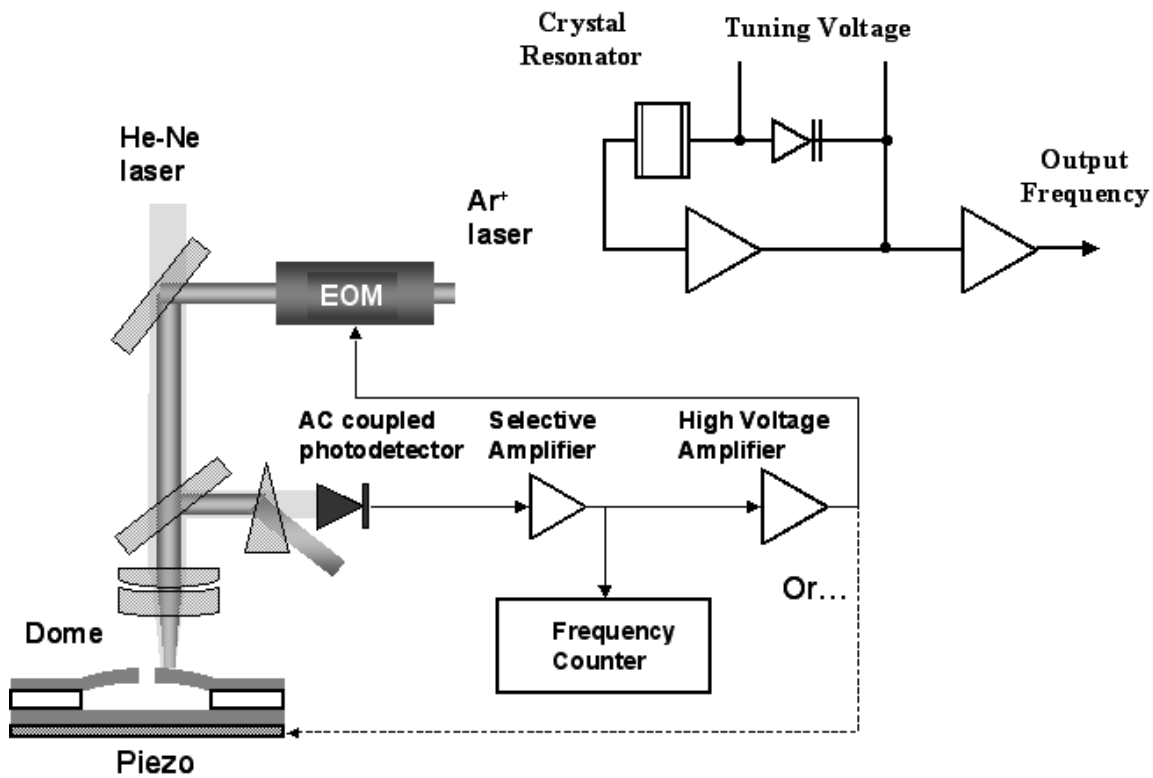Fig.6 Frequency stability of shell-based generator

Fig.7 Optical implementation of a positive feedback loop with the dome resonator as frequency-determining element.

CONCLUSION

Radio frequency shell-type polysilicon micromechanical resonators (bowed up out-of-plane) were fabricated employing the compressive stress incorporated in LPCVD-deposited film. Thermal stress introduced by the modulated laser light was demonstrated to be an affective driving mechanism for these dome-type resonators. All–optical operation was demonstrated employing two different wavelength laser beams for drivie and detection. The local nature of the laser actuation technique allows us to access modes of vibration that are not easily seen using a piezo-electric or capacitive drive. Mode identification was achieved by monitoring the phase shift between drive signal and detected motion at different locations. Finally, a prototype of a frequency generator was built implementing positive feedback, and demonstrated a frequency stability of better than 1 ppm.

ACKNOWLEDGMENTS

REFERENCES

[1] C. T.-C. Nguyen, *Digest of Papers*, Topical Meeting on Silicon Monolithic Integrated Circuits in RF Systems, Sept. 12-14, pp. 23 (2001)

[2] Mike Golio *The RF and Microwave Handbook,* CRC Press2001 pp.6-10

[3] B.A. Warneke, M.D.Scott, B.S. Leibovitz, Z. Lixia, C.L. Bellew, J.A. Chediak, J.M.Kahn, B.E. Boser, K.S.Pister Proceedings of First IEEE International Conference on Sensors; Piscataway, NJ, USA 1510-15 vol.2 (2002)

[4] M.J Madou- *Fundamentals of Microfabrication*

[5] J. R. Clark, W.-T. Hsu, and C. T.-C. Nguyen, *Tech. Digest*, IEEE Int. Electron Devices Meeting, San Francisco, California, Dec. 11-13, 2000, pp. 399.

[6] XMH Huang, CA Zorman, M. Meregany, M.L. Roukes, Nature **421** 496 (2003)

[7] K.Y. Yasumura, T.D.Stowe, E.M. Chow, T. Pfafman, T.W. Kenny, B.C. Stipe and D. Rugar, Journal of Microelectromechanical Systems, **9**, 117 (2000)

[8] R. Lifshitz, M.L. Roukes, Phys. Rev. B **61,** 5600 (2000)

[9] B.H. Houston, D.M. Photiadis, M.H. Marcus, J.A. Bucaro, X. Liu and J.F. Vignola Applied Phys. Lett. **80,** 1300 (2002)

[10] J. Yang, T. Ono, M. Esashi Applied Phys. Lett. **77**, 3860 (2000)

[11] K.L. Aubin, M. Zalalutdinov, R.B. Reichenbach, B.H. Houston, A.T. Zehnder, J.M. Parpia, H.G. Craighead "Laser Annealing for high-Q MEMS Resonators" – Proceedings of the present Symposium

[12] L. Seungbae, M.U. Demirci and Clark T.-C. Nguyen, *Digest of Technical Papers,* the 11th Int. Conf. On Solid-State Sensors and Actuators (Transducers'01), Munich, Germany, June 2001, pp. 1094

[13] T. Mattila, O. Jaakkola, J. Kiihamaki, J. Karttunen, T. Lamminmaki, P. Rantakari, A. Oja, H. Seppa, H. Kattelus, I. Tittonen, Sensors and Actuators A 97-98 497 (2002)

[14] T. Mattila, J. Kiihamaki, T. Lamminmaki, O. Jaakkola, P. Rantakari, A. Oja, H. Seppa, H. Kattelus, I. Tittonen, Sensors and Actuators A 101 1 (2002)

[15] Carr D., Craighead H., J. Vac. Sci. Technol. B 15(6) 2760 (1997)

[16] R. Ilic, D. Csaplewski, M. Zalalutdinov, H.G. Craighead, P. Neuzil, C. Campagnolo, C. Batt , Journal of Vac. Sci. & Tech. B **19**, 2825 (2001)

[17] A.N. Cleland, M.L. Roukes Nature **392**, 160 (1998)

[18] Z. Zhang, P.C. Hammel, Solid State Nuclear Magnetic Resonance **11**, 65 (1998)